THESIS FOR THE DEGREE OF LICENTIATE OF ENGINEERING IN SOLID AND STRUCTURAL MECHANICS

Mechanical track deterioration due to lateral geometry irregularities

KALLE KARTTUNEN

Department of Applied Mechanics
CHALMERS UNIVERSITY OF TECHNOLOGY
Göteborg, Sweden 2012

Mechanical track deterioration due to lateral geometry irregularities
KALLE KARTTUNEN

Thesis for the degree of Licentiate of Engineering 2013:02
ISSN 1652-8565
Department of Applied Mechanics
Chalmers University of Technology
SE-412 96 Göteborg
Sweden
Telephone: +46 (0)31-772 1000

Cover:
Predicted response of the outer wheel on the leading axle of a freight wagon with Y25-bogies negotiating a 438 metre radius curve. The solid line indicates predicted RCF damage (scale on the left axis) and the dotted line lateral position of wheel/rail contact point (scale on the right axis). Grey areas indicate predicted RCF (positive on the left vertical axis) or wear (negative) according to a wear number based criterion.

Chalmers Reproservice
Göteborg, Sweden 2012

Mechanical track deterioration due to lateral geometry irregularities
Thesis for the degree of Licentiate of Engineering in Solid and Structural Mechanics
KALLE KARTTUNEN
Department of Applied Mechanics
Chalmers University of Technology

Abstract

This thesis deals with how a degraded track geometry influences further degradation of the geometry and the formation of rolling contact fatigue (RCF) and wear of rails. The overall objective is optimisation of railway maintenance. For this, further understanding and quantification of the deterioration of track components are needed.

Dynamic multibody simulations have been performed featuring different wagons, and a track with different curve radii and different levels of track geometry degradation. With the resulting wheel/rail interaction degradation indicators are evaluated. Increased track shift forces are considered as an indicator of further track geometry degradation. Two different RCF indices (one shakedown map based and one wear number based) are used to quantify surface degradation of rails.

Measured lateral track irregularities were found to follow a normal distribution reasonably well. Furthermore, the standard deviation of track shift forces was shown to have a linear relationship with the standard deviation of the lateral irregularities.

For large curve radii an increase of the level of lateral irregularities increases the length of rail affected by RCF. The opposite is predicted for small curve radii where the length of rail affected by RCF decreases with increasing levels of lateral irregularities. For very small curve radii it was shown that the degradation mechanism shifts from pure wear for low levels of lateral irregularities to a mixed wear/RCF degradation for higher levels of lateral irregularities. Amplification of lateral irregularities in different wavelength spans revealed that an amplification of longer wavelengths (between 10–50 metres) had the largest influence on the length of rail affected by RCF in shallow curves.

A correlation study between predicted tangential wheel/rail contact forces and lateral irregularities (amplitudes of the irregularities, first order derivatives and second order derivatives) was carried out. No significant correlation was found.

Keywords: Railway track geometry, track irregularities, track maintenance, multibody dynamics simulations, rolling contact fatigue, wear

Preface

The work presented in this thesis has been carried out between October 2010 and December 2012 at the Department of Applied Mechanics at Chalmers University of Technology. It is part of the project MU27 "Progressive degradation of wheels and rails" within the Swedish National Centre of Excellence in Railway Mechanics (CHARMEC).

Acknowledgements

First of all I would like to give my sincere gratitude to my supervisor Elena Kabo and co-supervisor Anders Ekberg. I am not only thankful for their guidance, expertise and feedback, but also for making the work both interesting and fun.

I would also like to thank the members of the MU27 reference group: Viktor Berbyuk, Per Gelang, Simon Gripner, Roger Lundén, Arne Nissen, Jon Sundh and Thomas Svensson. Furthermore, I want to thank the members of the parallel CHARMEC project MU26: Emil Gustavsson, Ann-Brith Strömberg and Michael Patriksson (who is also a co-supervisor for this project). Also many thanks to Ingemar Persson for his valuable help with GENSYS.

Thanks also to the colleagues on the 3rd floor of the "Nya Maskinhuset" and especially to Dr. Anders T. Johansson who had the misfortune to have to share an office with me (and having the fortune to be tortured with fragments from good old "GBG punkdängor").

Göteborg, December 2012

Kalle Karttunen

Thesis

This thesis consists of an extended summary and the following appended papers:

Paper A K. Karttunen, E. Kabo, and A. Ekberg, A numerical study of the influence of lateral geometry irregularities on mechanical deterioration of freight tracks, *Proceedings of the Institution of Mechanical Engineers, Part F: Journal of Rail and Rapid Transit* 226.6 (2012), 575–586

Paper B K. Karttunen, E. Kabo, and A. Ekberg, The influence of track geometry irregularities on rolling contact fatigue (2012), Submitted for international publication

The appended papers were prepared in collaboration with co-authors. For **Paper A** and **Paper B** the author of this thesis was responsible for the major progress of the work in preparing the papers, i.e., took part in planning the papers, carried out the numerical analyses, and had the main responsibility for writing the papers.

The author has also taken part in the following work (which is not appended in this thesis).

A. Ekberg, E. Kabo, K. Karttunen, B. Lindqvist, R. Lundén, T. Nordmark, J. Olovsson, O. Samuelsson and T. Vernersson, Identifying root causes of heavy haul wheel damage phenomena, to be presented at the 10th International Heavy Haul Conference (IHHA 2013), Feb. 4–6 2013, New Delhi, India, 2013, 8 pp.

Contents

Abstract i

Preface iii

Acknowledgements iii

Thesis v

Contents vii

I Extended Summary 1

1 Introduction 1
1.1 Background . . . 1
1.2 Aim . . . 2
1.3 Limitations . . . 2

2 Numerical modelling 3
2.1 Simulation tools . . . 3
2.2 Vehicle models . . . 3
2.2.1 Iron ore wagon . . . 4
2.2.2 Freight wagon . . . 5
2.2.3 Generic locomotive . . . 6

3 Degradation of track geometry 6
3.1 Definition of track geometry . . . 6
3.2 Quantification of degraded track geometry . . . 7
3.2.1 Isolated defects . . . 7
3.2.2 Track quality measures . . . 8
3.2.3 Track shift forces . . . 9
3.3 Characteristics of track geometry degradation . . . 10

4 Degradation of rails 11
4.1 Surface rail defects . . . 11
4.1.1 Head checks . . . 11
4.1.2 Plastic deformation and wear . . . 12
4.2 Models for prediction of RCF . . . 12
4.3 Factors influencing rail degradation . . . 15

5 RCF prediction directly from track irregularities **17**

6 Summary of appended papers **18**

7 Concluding remarks and future work **19**

References **20**

II Appended Papers A–B **23**

Part I
Extended Summary

The intention of this extended summary is to present the main results from the two appended papers and to place them within a broader context together with results and findings from other related studies in the literature.

1 Introduction

1.1 Background

Maintenance of railways is a cornerstone in safe and reliable passenger and freight transportation. If maintenance is neglected, not performed properly, or performed too late the consequences could range from more extensive and expensive maintenance actions to fatal accidents. An additional and less severe consequence of bad maintenance is that the train ride may become less pleasant for passengers.

The total length of track in Sweden was 12077 kilometres in 2008 [44] which consequently is the length of track that had to be maintained. To be able to perform the maintenance actions at optimum time and with an optimum amount of efforts would lead to great savings.

In general maintenance actions can be divided into two areas: corrective and preventive. Corrective maintenance is defined as actions taken when a fault has occurred and preventive maintenance as actions taken before a fault has occurred. Corrective maintenance is typically more costly than preventive maintenance, experience from industry indicates at least a three-fold increase in costs [12]. Preventive maintenance can be further divided into two sub-areas: condition based and predetermined maintenance [1].

Typical maintenance actions that can be taken are tamping, ballast regulation, ballast stabilising, rail grinding, joint straightening, and ballast cleaning [13]. The maintenance actions mainly related to track geometry degradation and rail degradation are tamping and rail grinding. The deterioration of the track geometry is manifested as development of track geometry irregularities. A remedy is tamping (lining) where the track geometry is restored into its nominal geometry by shifting the track both vertically and laterally, and if necessary adding and tamping the ballast.

Deterioration of rails manifests itself in e.g. wear, corrugation and fatigue. In all mentioned cases grinding is used as a maintenance action. In the case of wear and corrugation the aim is to restore the shape of the rail profile. In the case of fatigue (more accurately surface initiated rolling contact fatigue (RCF)) the aim of grinding is to remove the layer of material with RCF cracks. The grinding can either be preventive or corrective [18]. In preventive grinding the rails are ground regularly to minimise the risk of cracks becoming substantial defects. Preventive grinding has also the positive effect that the rail profile is restored to a favourable shape which controls contact stresses, creepage, and rail surface roughness [7, 33]. This minimises the crack initiation and propagation

rates. Corrective grinding (or milling) is performed to prevent the risk of rail breaks if individual RCF cracks or rail sections subjected to RCF are detected.

To optimise the predetermined maintenance, predictive models of track and rail deterioration are needed. These predictive models could be probabilistic, mechanistic or empirical [1]. In this work the aim is to develop mechanistic or empirical models of deterioration (or a combination of these two).

Multibody simulations of the train/track interaction has been employed as the main tool to study the degradation of track and rails. The starting point is a degraded track geometry which is employed in multibody simulations. With the resulting wheel/rail interaction parameters from the simulations, different measures of degradation can be evaluated. By using different levels of degraded track geometry, from a newly tamped track (with low or no degradation) to a track being worse than the currently allowed track quality, the whole degradation cycle of a track can be evaluated.

1.2 Aim

The main aim of the PhD-project, of which this thesis is one part, is to develop predictive models of material deterioration of rails and wheels. The predictive models should give valuable help in maintenance optimisation and/or in maintenance planning. The outline of the project aims can broadly be divided into four parts:

1. To identify current degradation models.
2. To identify how deterioration of wheels and rails can be related to operational conditions.
3. To quantify the effects of altered operational conditions on track and wheel degradation.
4. To extract operational load spectra and resulting damage spectra.

In the present thesis the focus has been on the degradation of rails (and track).

1.3 Limitations

The first limitation of this thesis is the use of multibody dynamics simulations. The accuracy of these simulations is directly linked to the accuracy of the numerical model. The wagon models employed have been verified as described in the literature [4, 5, 23]. Still results obtained from simulations will differ from the "real" values. Some of the reasons behind this are the uncertainty of friction coefficients, manufacturing tolerances and the simplified assumption of rigid bodies in the numerical models. Another limitation in this thesis is the use of nominal wheel and rail profiles. This was employed to keep the number of variables in simulations at manageable levels. A drawback of this simplification is that the employed wheel/rail combination is prone to two-point contact (i.e. two simultaneous contact points between the wheel and the rail).

Nevertheless, the general conclusions drawn regarding the influence of degraded track geometry on further degradation of the track and rails with the aid of the numerical simulations should be valid. A motivation for this is that the simplifications should give

errors that are fairly independent of the track geometry. One could argue that, e.g. for the case of two-point contact this is not the case. However at such lateral wheel displacement the loading will be severe regardless of the two-point contact. In essence the difference will thus be in the magnitude of the trend.

2 Numerical modelling

2.1 Simulation tools

GENSYS [17] is a multibody dynamics simulation package specialised on train/track dynamics. Quasi-static, modal, frequency-response and time-domain analyses can be performed. In this thesis mainly time-domain analyses were performed (sometimes with an initial quasi-static analysis to serve as input to a subsequent time-domain analysis). The simulation package also includes supporting programs, e.g. for the generation of wheel/rail geometric functions and generation of track irregularity input files from measured irregularities. However, the track irregularity input files used in this thesis were generated by in-house Matlab scripts. Furthermore, post-processing of results was performed in Matlab.

2.2 Vehicle models

Three vehicle models have been employed in the multibody dynamics simulations: an iron ore wagon with three-piece bogies, a freight wagon with Y25-bogies, and a generic locomotive. Brief descriptions of the wagons are provided in the following sections. Table 2.1 shows the general vehicle properties. In the iron ore and freight wagons damping is achieved by friction, e.g. side bearers, centre-pivot/plates, friction wedges (in the

Table 2.1: Vehicle properties [4, 5, 17, 23].

	Heavy haul wagon	Freight wagon	Generic locomotive
Designation	Kockums Industrier Fammoorr^{050}	Kockums Industrier Smmnps^{951}	GENSYS
Length between centre line of couplers	10 300 mm	14 240 mm	N/A
Bogie type	three-piece	Y25-TTV	N/A
Bogie c/c distance	6 744 mm	9 200 mm	13 000 mm
Axle bogie distance	1 778 mm	1 800 mm	3 000 mm
Wheel diameter	915 mm	920 mm	1 000 mm
Total height	3 640 mm	1 800 mm	N/A
Tare weight	21.6 tons	20.3 tons	total 80 tons
Load capacity	102 tons	79.7 tons	

three-piece bogie) and Lenoir links (in the Y25-bogie). In the locomotive viscous damping is employed.

For all vehicle models a standard (in Sweden) track gauge of 1435 mm is employed. The employed friction coefficient in the wheel/rail contact is 0.4 unless otherwise stated.

2.2.1 Iron ore wagon

The iron ore wagon is a specialised wagon for the Iron Ore Line in northern Sweden. The maximum axle load is 30 tons and when loaded the maximum speed of the wagon is 60 km/h. The iron ore wagon has three-piece bogies (Amsted Rails M976 Motion Control®) as shown in Figure 2.1.

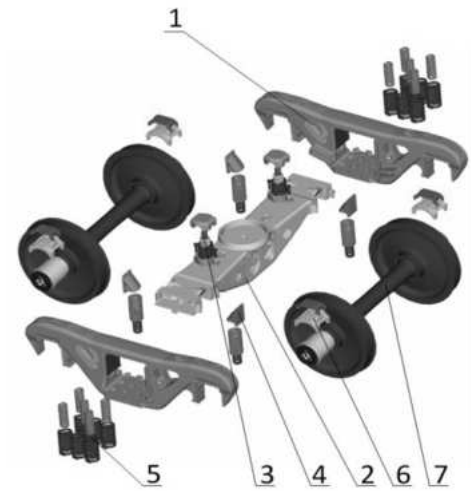

Figure 2.1: *Assembly of a three-piece bogie used in the iron ore wagon (from [5]). See text for a description of the numbered parts.*

The main parts in Figure 2.1 are:

1. Side frame – Connected to the bolster (2) with the coil spring assembly (5) and to the wheelset (7) with the adapter (6).
2. Bolster – The central plate on the bolster connects the bogie to the carbody.
3. Side bearer – Carries some of the load from the car body. Increases the stability of the vehicle due to increased damping in the longitudinal direction.
4. Friction wedge – Wedge between bolster and side frame which by friction provides damping.
5. Coil spring assembly – The main suspension of the bogie.
6. Adapter – Connects the wheelset (via a bearing) with the side frame and provides an elastic coupling in lateral and longitudinal directions.
7. Wheelset – Wheel profile UNO-WP-4.

Nominal rail profiles 50E3 with an 1:30 inclination are employed. The numerical model of the vehicle was developed by Bogojević [4, 5].

2.2.2 Freight wagon

The freight wagon is modelled after a steel ingot transport wagon. The maximum axle load is 25 tons and the maximum speed when fully loaded is 100 km/h. The bogies are modified Y25-bogies (Y25-TTV) and the main parts are (see also Figure 2.2):

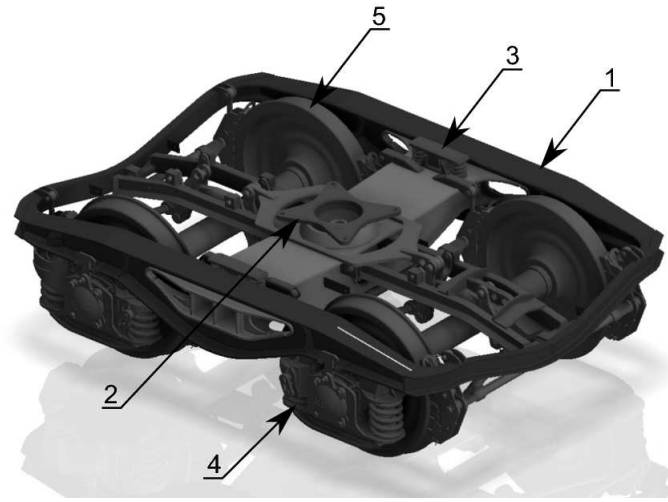

Figure 2.2: *Y25-bogie of the freight wagon. See text for an explanation of the parts (courtesy of Igor Antolovic at Kockums Industrier AB).*

1. Bogie frame
2. Centre-pivot – Transfers the main part of the loads from the carbody to the bogie. The centre-pivot can be regarded as a spherical plain bearing which enables rotation in all directions between the bogie and carbody.
3. Side bearer – Carries some of the load from the car body. Increases the stability of the vehicle due to increased damping in the longitudinal direction. Furthermore they will reduce the roll of the carbody.
4. Primary suspension – Load dependent vertical damping is provided by the so called Lenoir link.
5. Wheelset – Wheel profile EN S1002t32.5.

Nominal rail profiles 50E3 with an 1:30 inclination are employed. The model was originally developed and verified by Jendel [23]. Since then the model has been modified to take advantage of new functionalities of the simulation package.

2.2.3 Generic locomotive

The locomotive is a generic model of a two bogie railway vehicle (Bo'Bo') as included in the GENSYS simulation package. The main difference between the locomotive model and the two other models is that the damping in the locomotive model is achieved by viscous damping in contrast to friction damping in the other models. The axle load of the locomotive is 20 tons. Nominal wheel profiles (EN S1002t32.5) and nominal rail profiles UIC60 with 1:30 inclination are employed. Results from multibody simulations employing the generic locomotive model are only presented in this extended summary (i.e. no results using this model are presented in **Paper A** and **Paper B**).

3 Degradation of track geometry

3.1 Definition of track geometry

The track geometry can be described by the nominal geometry and irregularities. The nominal track geometry consists of vertical curvature, horizontal curvature, gradient (i.e. slope of track), track gauge and cross level (cant). Track irregularities are defined as the deviation of the actual track geometry from the nominal (designed) track geometry.

Definitions of track geometry measures according to [38] are as follows:

- Longitudinal level or vertical alignment: vertical deviation of the running table[1] from the reference line[2]. Measured for both rails.
- Lateral alignment or alignment: lateral deviation of both rails measured from a point between 0 to 14 mm below the running surface[3], see also Figure 3.1.
- Track gauge: track gauge is the shortest distance between the rails measured between 0 to 14 mm below the running surface, see also Figure 3.2.
- Cross level: cross level is evaluated from the angle between the running surface and horizontal reference plane. It is expressed as the vertical distance between the rails for a hypotenuse of 1500 mm for a nominal gauge of 1435 mm. For curved tracks cross level is often referred to as cant.
- Twist: the algebraic difference between two cross levels taken a defined distance apart.

Missing from the above list are vertical curvature, horizontal curvature and gradient. In this work, instead of curvatures, the curve radius is presented (i.e. the inverse of the curvature). Furthermore, vertical and lateral track irregularities are here defined as the deviation (in their respective direction) between the track's centreline and the reference centreline (i.e. as the average deviation of both rails).

[1] Upper surface of the head of the rail.
[2] Mean position.
[3] Surface tangential to running tables of the left and right rails.

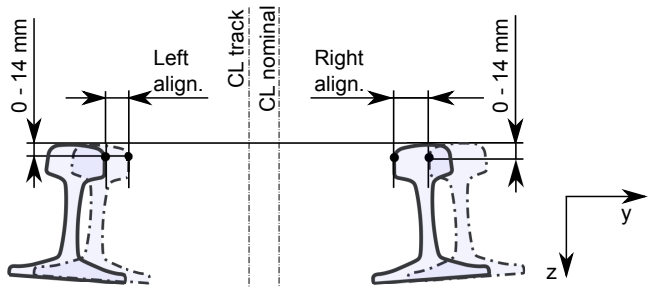

Figure 3.1: *Lateral alignment as defined in [38]. Dash-dotted rail profile represents the nominal (mean) position of the rail.*

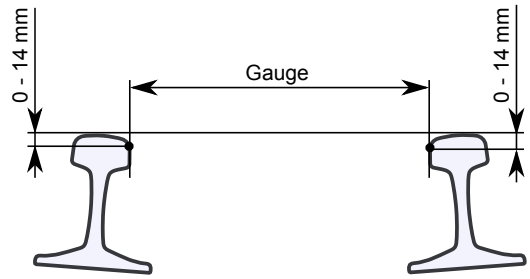

Figure 3.2: *Track gauge as defined in [38].*

3.2 Quantification of degraded track geometry

A number of track geometry degradation measures are defined in norms and standards. These norms and standards are historically specific for each country. In this section permissible levels for isolated defects and track qualities are given as defined in European standards (which are, or are in progress to become, national standards for many European countries). In general the purpose of the permissible levels of the isolated defects are to ensure that the safety is not jeopardised whilst the permissible levels for track quality can be seen as measures to ensure that the ride comfort does not become too bad.

3.2.1 Isolated defects

A classification of isolated track geometry defects is given in [39]. The isolated defects are divided into three groups based on the severity of the defect and on the time scale when mitigating actions have to be taken to correct the defect. The three groups are:

- Immediate Action Limit: if this value is exceeded then mitigation actions have to be taken immediately (e.g. immediate tamping, closing of the line or reduced speed limits).
- Intervention Limit: if this value is exceeded then corrective maintenance has to be performed in order to ensure that the immediate action limit is not reached before

the next inspection.
- Alert Limit: if this value is exceeded then correction of track geometry has to be considered in the regular planning of maintenance operations.

Of these, only the immediate action limits are given as binding values in the standard whereas the two other limits are provided as guidelines for maintenance planning. In Table 3.1 the immediate action limits and alert limits for lateral alignment are given. The immediate action limits are less stringent than current limits in Sweden as specified in [19]. The alert limit values are roughly half of the immediate action limit values.

Table 3.1: Immediate action limits and alert limits for lateral aligment at an isolated defect with a wavelength of 3 to 25 metres [39].

Speed [km/h]	Immediate action limit	Alert limit
	Zero to Peak value [mm]	Zero to Peak value [mm]
$v \leq 80$	22	12 to 15
$80 < v \leq 120$	17	8 to 11
$120 < v \leq 160$	14	6 to 9
$160 < v \leq 230$	12	5 to 8
$230 < v \leq 300$	10	4 to 7

3.2.2 Track quality measures

A common quantification measure of track geometry quality is the standard deviation of irregularities over a specified length. The standard deviation is calculated as:

$$s = \sqrt{\frac{1}{n-1}\sum_{i=1}^{n}(\delta_i - \overline{\delta})^2} \tag{3.1}$$

where δ_i is the measured irregularity, $\overline{\delta}$ is the mean value, and n is the number of measurements.

Maximum permissible values of the standard deviation for track irregularities are related to the maximum line speed and quality class of the track. As an example, prEN 13848-6 [40] limits of the standard deviations for alignment (in a wavelength span of 3 to 25 metres evaluated over a length of 200 metres) are presented in Table 3.2. Limits and track quality classes were obtained by surveying track qualities around Europe. The track quality classes are defined as:

- Class A: best 10% of the cumulative distribution of the measured standard deviations
- Class B: between 10% and 30%
- Class C: between 30% and 70%
- Class D: between 70% and 90%
- Class E: above 90%

Table 3.2: Limit of standard deviation of alignment (in [mm]) according to [40] (average of the standard deviations of left and right rails).

Speed [km/h]	Track quality class				
	A	B	C	D	E
$v \leq 80$	< 0.90	1.25	1.95	2.7	> 2.70
$80 < v \leq 120$	< 0.50	0.70	1.05	1.45	> 1.45
$120 < v \leq 160$	< 0.45	0.55	0.75	1.00	> 1.00
$160 < v \leq 230$	< 0.40	0.50	0.70	0.90	> 0.90
$230 < v \leq 300$	< 0.35	0.40	0.50	0.65	> 0.65
$v > 300$	N/A	N/A	N/A	N/A	N/A

3.2.3 Track shift forces

The lateral track shift force is the total lateral force induced by the wheelset on the track (see Figure 3.3). High track shift forces may lead to large permanent deformations of the track. Therefore a safety limit criterion has been proposed [45]. According to this criterion the 2 metre moving average of the track shift force $Y_{2\mathrm{m}}$ [kN] may not exceed

$$Y_{2\mathrm{m}} \leq K \left(10 + \frac{2Q_0}{3} \right) \tag{3.2}$$

where $K = 0.85$ for freight wagons and $K = 1$ for passenger vehicles. Furthermore, Q_0 [kN] is the static vertical wheel force.

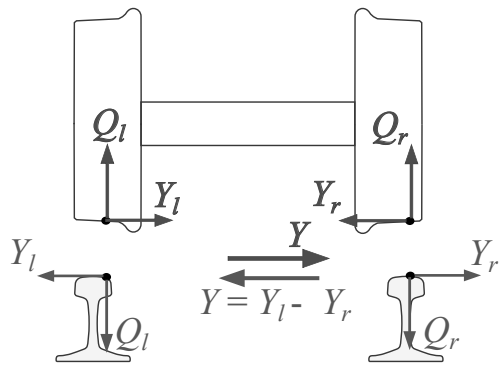

Figure 3.3: *Definition of lateral track shift force Y, vertical wheel force (Q_l, Q_r; left and right respectively) and lateral wheel force (Y_l, Y_r). View in the rolling direction of the wheelset.*

3.3 Characteristics of track geometry degradation

Track geometry degradation is caused by a re-arrangement of ballast particles due to loads and vibrations from passing train. Furthermore, the loss of angularity of the ballast particles due to tamping actions lead to increased deterioration rates over time since the interlocking between the particles is not as effective when the ballast stones become more rounded [35].

The characteristics of track geometry deterioration was investigated in [37]. Some of the conclusions are reiterated below:

- Both the vertical and lateral alignment deteriorate linearly with tonnage or time between maintenance operations after the first initial settlement. This trend is not always seen for sections with high deterioration rates.
- The rate of deterioration is very different from section to section even for apparently identical sections carrying the same traffic.
- The rate of deterioration appears to be a constant parameter for a section of track regardless of the quality achieved by the maintenance machine.

The first point in the above list is illustrated in Figure 3.4 where it is illustrated how the fast deterioration rate after tamping becomes more or less linear after some time. The two first points in the list have been demonstrated in [2] for a Portuguese rail line. Furthermore the second point is validated in [3] where a distribution of longitudinal deterioration rates for the Iron Ore Line in Sweden is presented. Some locations on the line have exceptionally high deterioration rates in comparison to the main part of the line. Furthermore in [3], seasonal variations in track geometry faults that have to be corrected are found.

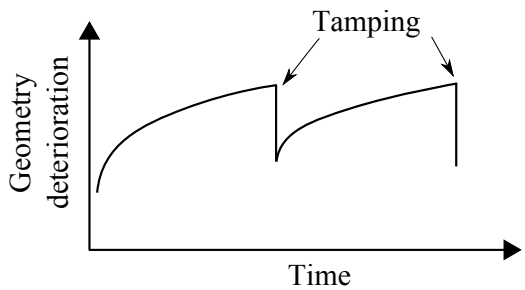

Figure 3.4: *Schematic illustration of track geometry deterioration over time.*

In [13] mean deterioration rates of track geometry are presented. Vertical irregularities deteriorate at a mean rate between 0.7 to 1.4 mm per 100 MGT (million gross tonnes). In comparison the lateral mean deterioration rate is smaller, between 0.3 to 0.8 mm per 100 MGT. In cases where both the mean vertical and mean lateral deterioration rates are presented the vertical deterioration rate is between 1.4 to 3.7 times higher than the lateral deterioration rate. For the Iron Ore Line similar longitudinal deterioration rates have been presented in [3].

In [20, 21] studies on which vehicle parameters that influence the vertical deterioration of track geometry are presented. The parameters with the greatest influence are train speed and suspension damping. Total mass of the vehicle (and the load) also had an influence on the deterioration although not as great as speed and damping. Unsprung mass and suspension stiffness had little or no influence on the vertical deterioration of track geometry.

In **Paper A** track shift forces were evaluated for different levels of lateral deterioration of the track geometry. A roughly linear relationship between the standard deviations of the lateral irregularities and track shift forces was found. Furthermore, a variation in the wheel/rail friction coefficient did not give any significant influence on predicted track shift forces.

4 Degradation of rails

4.1 Surface rail defects

In this section several types of surface damage of rails are described. The same types of surface defects on a rail may have different denotations in the literature. References used in this section are [7, 9, 14, 32].

4.1.1 Head checks

Head check cracks are manifested as closely spaced cracks of similar direction and size. They are caused by a combination of high normal and tangential stresses at the wheel/rail contact typically at the gauge corner. The stresses cause severe shearing of the surface layer of the rail that leads to fatigue and/or exhaustion of the ductility of the material. The initial microscopic cracks propagate at a shallow angle through the plastically deformed (anisotropic) material in the surface layer. When the crack has grown to a depth where there are no significant plastic deformation of the (isotropic) material different types of damage may develop depending on in which direction crack propagation continues. If the cracks branch towards the surface (or merge with other cracks), parts of the surface material may break loose. This is often called spalling and is regarded as a relatively harmless form of damage. If instead the crack grows and propagates downwards the end result may be a transverse failure of the rail. Needless to say, a transverse failure of the rail may have serious consequences. The depth below the surface where the microstructure becomes isotropic has been shown experimentally to be between 1 to 5 mm depending on the hardness of the rail [22] (the harder rails generally have a smaller depth of plastically deformed material given the same operational loading).

Crack mouths are generally oriented perpendicularly to the acting creep forces [32]. In curves the cracks are oriented at an angle due to the combined influence of lateral and longitudinal creep forces. Head checking at the gauge corner is often called gauge corner cracking (GCC), see also Figure 4.1. These cracks may occur on long rail lengths (e.g. throughout a curve) or they may be found in clusters (e.g. due to track irregularities) [32].

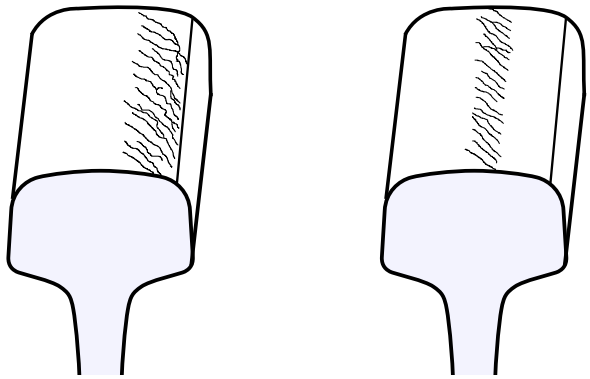

(a) (b)

Figure 4.1: *Typical appearance of (a) head checks on the gauge corner of the high rail and (b) head checks on the top surface.*

4.1.2 Plastic deformation and wear

Due to the high contact forces in the wheel/rail interface, plastic deformation of the rail is common. In curves, the plastic deformation may lead to a lip (or bulge) below the gauge corner of the outer rail [34]. On the inner rail plastic flow towards the field side may occur, see e.g. [46]. Plastic deformation may also occur on the top of the inner rail.

Wear is closely related to RCF and can be seen as a competing damage mechanism. Wear usually dominates at small radii curves and RCF at shallow curves [41]. Wear is usually the dominant damage mechanism for curves up to some 700 to 1000 metres, and RCF is the dominant damage mechanism for curves with a radius between some 500 to 5000 metres [36]. As it can be noted there is quite an overlap in the curve radius ranges where wear and RCF are dominant damage mechanisms. Reasons for this is the influence of the running gear of operating vehicles and rail/wheel lubrication. At sharp curves wear takes place at the gauge corner of the outer rail and on the top surface of the inner rail. Different wear mechanisms may affect the gauge corner and top surface [34]. For the gauge corner severe wear is typically the dominating mechanism and for the top surface mild wear is usually predominant. Furthermore, the difference in wear rate between the gauge corner and top surface may be as large as a factor of 10 [34].

Wear may be regarded as a track geometry irregularity if the gauge corner wear becomes substantial [14]. In such case the track gauge (see Section 3.1) increases.

4.2 Models for prediction of RCF

In this section two RCF prediction models are presented. Both models are related to surface initiated RCF which correspond, e.g. to head check formation as discussed in Section 4.1. In one of the models the influence of wear is included.

A prediction model for *surface* initiated RCF is presented in [10]. The RCF prediction

model sets out from the shakedown map [24] where surface initiated RCF is linked to the occurrence of plastic flow in the contact surface. An RCF index, FI_{surf}, is defined as the horizontal distance between the utilised friction coefficient and normalised vertical load in the shakedown map (see Figure 4.2) and can be formulated as:

$$FI_{\text{surf}} \equiv f - \frac{1}{\nu} = f - \frac{2\pi abk}{3|F_z|} \tag{4.1}$$

where a and b are the semi-axes of the presumed Hertzian contact patch, k the yield strength of the material in cyclic shear (in the thesis taken as 300 MPa) and $f = \sqrt{F_x^2 + F_y^2}/\sqrt{F_z^2}$ is the utilised friction coefficient with the tangential longitudinal F_x and lateral F_y wheel/rail contact forces, and the normal (vertical) wheel/rail contact force F_z (coordinate system is shown in Figure 3.1).

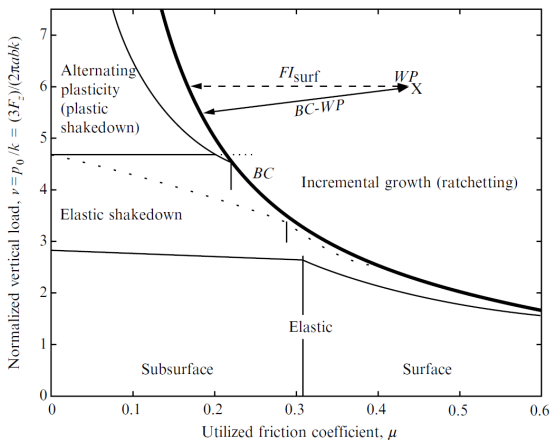

Figure 4.2: *Definition of FI_{surf} in the shakedown map (from [10]).*

Comparisons of predicted FI_{surf} values and experimentally found fatigue lives (from a full-scale roller rig, a full-scale linear test rig, and a twin-disk machine) indicated a Wöhler-like relationship [25]

$$FI_{\text{surf}} = 1.78 \cdot (N_{\text{f}})^{-0.25} \tag{4.2}$$

where N_{f} is the fatigue life. Equation 4.2 can be expressed as the surface RCF damage per cycle $D \equiv 1/N_{\text{f}}$, as

$$D = \frac{(FI_{\text{surf}})^4}{10} \quad \forall FI_{\text{surf}} \geq 0. \tag{4.3}$$

A different RCF prediction model is presented in [6]. Here a damage energy parameter based on the wear number, $T\gamma = F_x\gamma_x + F_y\gamma_y$ (where γ_x and γ_y are the creepages in longitudinal and lateral directions, respectively), is employed. $T\gamma$ represents the energy dissipated in the contact patch. Damage is predicted according to the relationship in Figure 4.3. The criterion states that no damage is predicted for $T\gamma \leq 15\,\text{N}$, an increase

of RCF damage in the interval $15\,\mathrm{N} < T\gamma \leq 65\,\mathrm{N}$, and a decrease of RCF damage for $65\,\mathrm{N} < T\gamma \leq 175\,\mathrm{N}$. Finally, for $T\gamma > 175\,\mathrm{N}$ wear is considered to be the dominating damage mechanism. The damage function was constructed by correlating measurements (of locations with RCF cracks) at six different sites (in the UK) to results from multibody simulations.

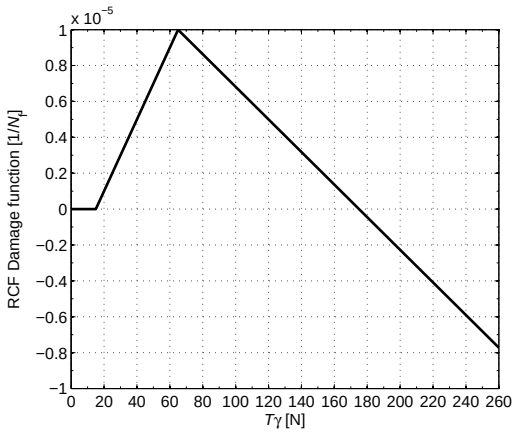

Figure 4.3: *Damage function for $T\gamma$.*

In [42] a classification of the severity of RCF based on both FI_{surf} and the wear number $T\gamma$ is presented . Figure 4.4 shows three areas where area 1 indicates high risk for RCF, area 2 indicates some risk for RCF, and area 3 indicates a low risk for RCF. It should be noted that the classification was derived for the inner wheel of the leading wheelset of a passenger train but it should also be applicable as a general guideline for the high rail in curves.

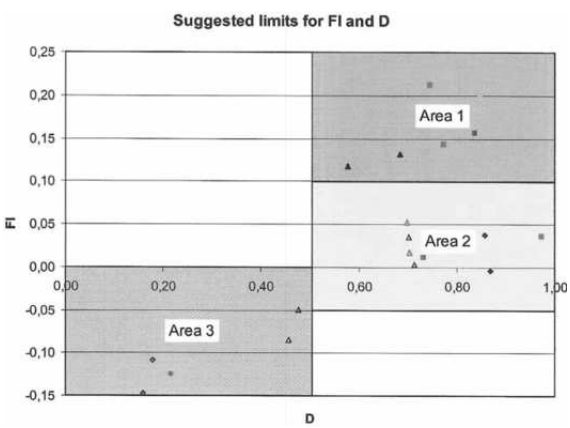

Figure 4.4: *RCF risk assesment map from [42]. FI is FI_{surf} and D is the relative wear number based RCF damage (D=1 equals the maximum value of the damage function).*

4.3 Factors influencing rail degradation

The common parameter in the shakedown map and the wear number based RCF prediction models is the tangential force. Curve radii and lateral track irregularities have a large influence on the tangential force.

The main global parameter that dictates the degradation of a rail is the curve radius. In general, the dominant degradation mechanism is wear for small curve radii and RCF for larger curve radii. An example of this can be seen in Figure 4.5 where length of rail affected by RCF or wear as predicted with the $T\gamma$-criterion is presented. For the high rail of the 438 metre radius curve wear is the dominating damage mechanism and for the 1578 metre radius curve RCF is the dominating damage mechanism. What constitutes a small or large curve radius in this context depends on vehicle properties and (deteriorated) track geometry. For a track geometry without any irregularities, a step-like relationship between curve radius and RCF can be expected (as shown in Figure 4.6). For decreasingly smaller curve radii there is a sudden jump from no predicted RCF over the length of the curve to RCF predicted for the whole curve (from a purely quasi static point-of-view). For the curve radius where the RCF "jump" takes place the tangential creep forces are just large enough to cause RCF. A similar reasoning may be made regarding the influence of curve radius on predicted wear where both creep forces and creepage has to be taken into account (if a wear number based wear criterion is considered). A closely related parameter is the primary yaw stiffness of a wagon. In [48] an investigation with a two-axle wagon showed that in small radius curves RCF increases with increased primary yaw stiffness.

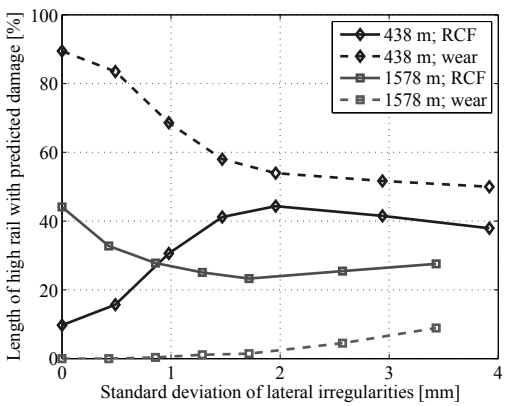

Figure 4.5: *Percentage of length of high rail where* $15\,N < T\gamma < 175\,N$ *(RCF) and where* $T\gamma \geq 175\,N$ *(wear) is predicted for a 438 metre and 1578 metre radius curves on the Iron ore line (see* ***Paper A*** *for a description of the curves) for freight wagon with Y25-bogies.*

The influence of lateral irregularities on RCF is mostly pronounced for curves with large radii. In these large radius curves a more laterally degraded track geometry leads to more RCF (see Figure 4.6 and **paper B**). Employing Eq. 3.1 in a wavelength span of 3 to 25 metres (see 3.2.2) on low and high levels of (filtered) irregularities employed in

the multibody simulations of **Paper B** gives standard deviations of about 0.6 mm and 1.1 mm, respectively. Relating these standard deviations to the track quality measures in Table 3.2 it can be noted that both standard deviations are high for the high speed lines while representing reasonable values for low speed lines. In [47] it is stated that for curves more shallow than 1800 metres improving lateral alignment is the primary RCF mitigation measure. For small curve radii where wear is the dominant damage mechanism an increase of lateral irregularities leads to a mixed wear/RCF damage on the rail. An example of this can be seen in Figure 4.5 where, for the high rail of the 438 metre radius curve, the length of wear affected rail decreases almost at the same rate as the length of RCF affected rail increases for increasing levels of lateral irregularities.

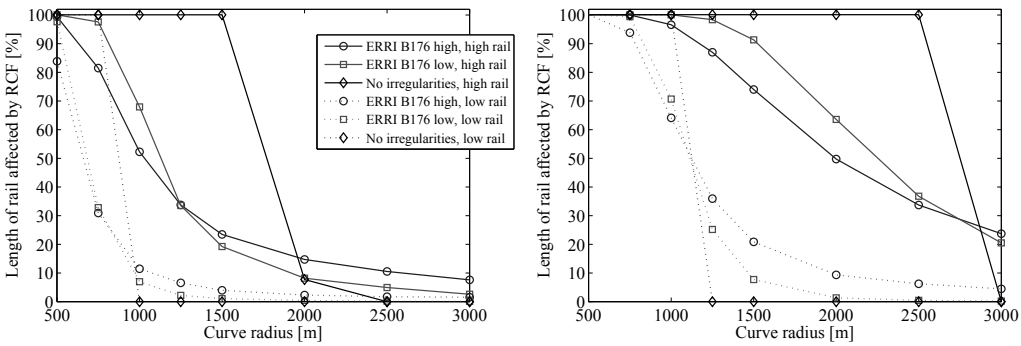

(a) *Freight wagon* (b) *Generic locomotive*

Figure 4.6: *Percentage of rail length with RCF as predicted by* FI_{surf}*. Cant deficiency of 39 mm for both vehicles.*

Increasing the cant deficiency is proposed as one RCF mitigation measure for curve radii between 1000 and 1800 metres [47]. The reasoning behind this is that an increased cant deficiency shifts the trailing wheelset of a bogie towards the high rail and thus lowers the angle of attack of the leading wheelset. This leads to smaller creep forces for the leading wheelset (i.e. reducing RCF) but increases the creep forces for the trailing wheelset (although not to a such extent that it will increase RCF significantly).

The influence of wheel conicity on RCF is studied in [48]. It is reported that a larger conicity leads to more RCF in large radius curves (in this case 1500 metres radius for a wagon with enhanced three-piece bogie). This is explained by the fact that a small offset in the lateral position of the wheelset causes larger longitudinal creep forces. For small radius curves an increased conicity increases the steering capability and thus less RCF is predicted. Naturally the opposite is predicted for reduced conicity.

The influence of hollow worn wheel profiles on wheel/rail contact stresses and RCF were studied in [15, 16]. Hollow worn wheels may lead to false flange contact and result in high contact stresses with the consequence of more RCF damage to the rail.

Also single track irregularities may influence the formation of RCF. In **Paper B** this influence was investigated. It was concluded that an irregularity with an amplitude of

6 mm and a length of less than 20 m was sufficient to cause RCF. The current alert limit for lateral alignment (see Table 3.1) is about 6 mm in irregularity amplitude for the highest line speeds. Thus RCF damage at single irregularities may form even if the alert limit is not reached.

The coefficient of friction between the wheel and rail also has a significant influence on the surface degradation of rails. Friction modifiers and lubrication are commonly used in curves to reduce both wear and RCF [8, 43]. Usually lubrication is applied to the gauge face and (less commonly) friction modifiers to the top of the rail. The friction coefficient also varies naturally. In wet conditions the coefficient of friction may be substantially lower than in dry conditions. In **Paper A** a study of the influence of the wheel/rail friction coefficient (varied between 0.3 and 0.6; and the same for both the right and left rail) showed that an increase of the friction coefficient generally leads to higher RCF damage magnitudes.

5 RCF prediction directly from track irregularities

To be able to perform more efficient maintenance, it would be desirable to be able to predict rail deterioration computationally efficiently. A step in such a direction would be the ability of predicting wheel/rail contact forces without having to perform multibody dynamics simulations. A proposed method is based on a system identification of the results from multibody dynamics simulations, see e.g. [30]. In [31] (which is inspired by the study in [29]) measured track irregularities are correlated with measured wheel/rail forces. The measurements were conducted in the DynoTRAIN project where a train was run on different test tracks. The track irregularities as well as the wheel/rail forces for wagons and locomotives were measured. Correlations are evaluated between all of the combinations of irregularity amplitudes, first and second order derivatives of these, and the standard deviation of wheel forces, maximum wheel forces, and 99.85 percentile of the wheel forces. The irregularity measures are also characterised by standard deviations, maximum values, and 99.85 percentiles. For vertical track irregularities and vertical wheel/rail forces the best correlations were achieved for first order derivatives [31]. Furthermore, in [31] lateral wheel/rail forces are correlated with first order derivatives of the lateral irregularities (filtered between 3 and 25 metres) where for a wagon the correlation coefficient is of roughly the same absolute magnitude as presented in **Paper B**. It should be noted that the correlation coefficients presented in [31] were calculated with the irregularities and wheel/rail forces as 99.85:th percentiles (in addition it is not clear from which test track the measurements originate and what the pertinent curve distribution is). Also in [26] measurements of wheel/rail forces are correlated with measured track irregularities. The measurements were performed with a high-speed passenger train with speeds up to 300 km/h. Lateral track shift forces (99.85 percentile) of the trailing axle of the bogie showed rather poor correlation with the lateral amplitudes.

In **Paper B** correlations between predicted tangential (i.e. lateral and longitudinal) wheel/rail contact forces in the track plane and lateral track irregularities are studied. The

main conclusion is that the best correlation is achieved between the magnitude of the first order derivatives of the lateral irregularities and tangential wheel/rail forces of the outer leading wheel in the first bogie. Correlations between the tangential wheel/rail forces and the amplitude of the irregularity, and the second order derivative of the irregularity were poor. Furthermore, the correlation depended on the curve radius where small radius curves produced higher correlation coefficients than large radius curves.

6 Summary of appended papers

Paper A, *A numerical study of the influence of lateral geometry irregularities on mechanical deterioration of freight tracks.* Measured track geometry and irregularities from the Iron ore line are employed in multibody dynamics simulations featuring two different vehicle models (Iron ore wagon with three-piece bogies and a freight wagon with Y25-bogies). The measured lateral irregularities were scaled to mimic different states of a laterally deteriorated track. Also the wheel/rail friction coefficient was varied between 0.3 and 0.6 (a nominal coefficient of friction of 0.4). A roughly linear relationship between the standard deviations of the lateral irregularities and track shift forces was found. Furthermore, a variation to the wheel/rail friction coefficient did not give any significant influence on the track shift forces. RCF was studied with both a shakedown map based criterion (FI_{surf}) and a wear number based criterion ($T\gamma$). At sharp curves the portion of the high rail where RCF is predicted decreases with increasing lateral track irregularities. For these sharp curves the damage shifts from pure wear for low levels of lateral irregularities to a mix of wear and RCF for higher levels of lateral irregularities. For shallow curves the length of rail affected by RCF increases for increasing levels of lateral irregularities. An increase of the friction coefficient generally leads to a higher RCF damage magnitudes.

Paper B, *The influence of track geometry irregularities on rolling contact fatigue.* Both single lateral irregularities and lateral irregularities generated from PSD:s are employed in multibody simulations featuring a freight wagon with Y25-bogies. Single lateral irregularities were applied to a straight track to study which irregularity amplitude and length that will cause RCF. The generated random lateral irregularities were applied to curves with radii ranging between 500 to 3000 metres. Similar results were obtained as in **Paper A** i.e. for shallow curves (radii larger than 1250 metres) the length of track affected by RCF increases with increasing levels of lateral irregularities. The 95:th percentile magnitude of FI_{surf} is not significantly affected by an increase in the level of lateral irregularities for curves with a radii of 2000 metres or less. Furthermore, lateral irregularities in wavelength spans (2–10 metres, 10–25 metres and 10–50 metres) have been amplified in these simulations. For curves larger than 1250 metres it was found that the amplification of the irregularities in the longer wavelength spans increased RCF the most (both in terms of length of track affected and the 95:th percentile of FI_{surf}). Also a correlation study between predicted tangential wheel forces in the track plane and lateral irregularities (amplitudes of the irregularities, first order derivatives and second order derivatives) was conducted. No significant correlation was found.

7 Concluding remarks and future work

In this thesis the influence of lateral track geometry irregularities on deterioration of rails and track geometry is investigated employing multibody dynamics simulations. The basic methodology used is to employ different levels of laterally degraded track geometry (i.e. lateral track irregularities) to investigate how track shift forces and RCF of rails are affected.

Measured lateral track irregularities were found to follow a normal distribution reasonably well. Furthermore, the standard deviation of track shift forces was shown to have a roughly linear relationship with the standard deviation of the lateral irregularities. A drawback with the linear relationship is that it is vehicle dependent.

The influence of the level of lateral track irregularities on RCF of rails differs depending on the curve radius. For large curve radii an increase of the level of lateral track irregularities gives an increase in the rail length affected by RCF. The opposite is predicted for small curve radii where the length of rail affected by RCF decreases with increasing levels of lateral track irregularities. For the small curve radii it was shown that the degradation mechanism shifts from pure wear for low levels of lateral irregularities to a mixed wear/RCF degradation for higher levels of lateral irregularities. Amplification of lateral irregularities in different wavelength spans revealed that an amplification of longer wavelengths (between 10–50 metres) had the largest influence on the length of rail affected by RCF in shallow curves.

A correlation study between lateral track irregularities and tangential wheel/rail contact forces as quantified by the amplitude of the irregularity, first and second order derivative of irregularities did not reveal any significant correlation.

Looking back to the aims of this project (see Section 1.2), the second point in the list is highly prioritised. This point concerning the deterioration of wheels, has more or less been omitted in this thesis and will have more focus in the continuation of the project (although it is the focus of another study in the project [11]). Furthermore, the influence of worn wheel and rail profiles on RCF will be studied. Prediction of wheel/rail contact forces with higher accuracy and more computationally efficient (i.e. without multibody dynamics simulations) could be a topic of interest for infrastructure managers. An approach where a system identification is performed from results of multibody dynamics simulations might be feasible here.

References

[1] M. Andersson, *Strategic planning of track maintenance – State of the art*, Report, Department of infrastructure, KTH, 2002, 61 pp., ISRN: KTH/INFRA/–02/035–SE.

[2] A. Andrade and P. Teixeira, Uncertainty in rail–track geometry degradation: Lisbon-Oporto line case study, *Journal of Transportation Engineering* 137.3 (2011), 193–200.

[3] I. Arasteh khouy, Optimization of track geometry maintenance – a study of track geometry degradation to specify optimal inspection intervals, Licentiate thesis, Luleå University of Technology, 2011, 98 pp., ISBN: 978-91-7439-276-0.

[4] N. Bogojević, P. Jönsson, and S. Stichel, Iron ore transportation wagon with three-piece bogies – simulation model and validation, The 7th international scientific conference heavy machinery (HM2011), June 29–July 2 2011, Vrnjačka Banja, Serbia, 2011, 6 pp.

[5] N. Bogojević et al., Dynamic behaviour of freight wagons with three-piece bogie on Swedish Iron Ore Line, 22nd International Symposion on Dynamics of Vehicles on Roads and Tracks (IAVSD2011), Aug. 14–19 2011, Manchester, UK, 2011, 6 pp.

[6] M. Burstow, *Whole life rail model application and development for RSSB – continued development of an RCF damage parameter*, Report, Derby, UK: Rail Safety & Standards Board, 2004, 74 pp.

[7] D. Cannon et al., Rail defects: an overview, *Fatigue and Fracture of Engineering Materials and Structures* 26.10 (2003), 865–886.

[8] D. Eadie et al., The effects of top of rail friction modifier on wear and rolling contact fatigue: full-scale rail-wheel test rig evaluation, analysis and modelling, *Wear* 265.9-10 (2008), 1222–1230.

[9] A. Ekberg and E. Kabo, Fatigue of railway wheels and rails under rolling contact and thermal loading – an overview, *Wear* 258.7-8 (2005), 1288–1300.

[10] A. Ekberg, E. Kabo, and H. Andersson, An engineering model for prediction of rolling contact fatigue of railway wheels, *Fatigue and Fracture of Engineering Materials and Structures* 25.10 (2002), 899–909.

[11] A. Ekberg et al., Identifying root causes of heavy haul wheel damage phenomena, to be presented at the 10th International Heavy Haul Conference (IHHA 2013), Feb. 4–6 2013, New Delhi, India, 2013, 8 pp.

[12] U. Espling, Maintenance strategy for a railway infrastructure in a regulated environment, PhD thesis, Division of Operation and Maintenance Engineering, Luleå University of Technology, 2007, 171 pp.

[13] C. Esveld, *Modern railway track*, 2nd ed., Zaltbommel, The Netherlands: MRT–Productions, 2001, 654 pp., ISBN: 90-800324-3-3.

[14] D. Fletcher, F. Franklin, and A. Kapoor, "Rail surface fatigue and wear", *Wheel – rail interface handbook*, ed. by R. Lewis and U. Olofsson, Cambridge, UK: Woodhead publishing limited, 2009, pp. 280–310, ISBN: 978-1-84569-412-8.

[15] R. Fröhling, A. Ekberg, and E. Kabo, The detrimental effects of hollow wear – field experiences and numerical simulations, *Wear* 265.9-10 (2008), 1283–1291.

[16] R. Fröhling, U. Spangenberg, and G. Hettasch, Wheel/rail contact geometry assessment to limit rolling contact fatigue initiation at high axle loads, *Vehicle System Dynamics* 50.supp 1 (2012), 319–334.

[17] GENSYS, URL: `www.gensys.se`.

[18] S. Grassie, Rolling contact fatigue on the British railway system: treatment, *Wear* 258.7-8 (2005), 1310–1318.

[19] S. Hammarlund, *Spårlägeskontroll och kvalitetsnormer – central mätvagn STRIX, BVF 587.02*, in Swedish, Banverket, 1997, 12 pp.

[20] H. Hawari, Minimising track degradation through managing vehicle/track interaction, PhD thesis, School of Urban Development, Queensland University of Technology, 2007.

[21] H. Hawari and M. Murray, Effects of train characteristics on the rate of deterioration of track roughness, *Journal of Engineering Mechanics* 134.3 (2008), 234–239.

[22] J. Jaiswal, *Characterisation of microstructural deformation as a function of rail grade*, Report D4.3.6, INNOTRACK, 2009, 30 pp.

[23] T. Jendel, Dynamic analysis of a freight wagon with modified Y25 bogies, MSc thesis, Deparment of Vehicle Engineering, KTH, 1997, 87 pp.

[24] K. Johnson, The strength of surfaces in rolling contact, *Proceedings of the Institution of Mechanical Engineers. Part C. Journal of Mechanical Engineering Science* 203.C3 (1989), 151–163.

[25] E. Kabo et al., Rolling contact fatigue prediction for rails and comparisons with test rig results, *Proceedings of the Institution of Mechanical Engineers, Part F: Journal of Rail and Rapid Transit* 224.4 (2010), 303–317.

[26] T. Karis, Track irregularities for high-speed trains, MSc thesis, KTH, Rail Vehicles, 2009, 111 pp., ISBN: 978-91-7415-547-1.

[27] K. Karttunen, E. Kabo, and A. Ekberg, A numerical study of the influence of lateral geometry irregularities on mechanical deterioration of freight tracks, *Proceedings of the Institution of Mechanical Engineers, Part F: Journal of Rail and Rapid Transit* 226.6 (2012), 575–586.

[28] K. Karttunen, E. Kabo, and A. Ekberg, The influence of track geometry irregularities on rolling contact fatigue (2012), Submitted for international publication.

[29] M. Li et al., On the use of second-order derivatives of track irregularity for assessing vertical track geometry quality, *Vehicle System Dynamics* 50.supp 1 (2012), 389–401.

[30] B. Luber, A. Haigermoser, and G. Grabner, Track geometry evaluation method based on vehicle response prediction, *Vehicle System Dynamics* 48.supp 1 (2010), 157–173.

[31] G. Lönnbark, Characterization of track irregularities with respect to vehicle response, MSc thesis, KTH, Rail Vehicles, 2012, 48 pp., ISBN: 978-91-7501-406-7.

[32] E. Magel, *Rolling contact fatigue: a comprehensive review*, Report DOT/FRA/ORD-11/24, Washington DC, USA: U.S. Department of Transportation – Federal railroad administration, 2011, 132 pp.

[33] E. Magel et al., The blending of theory and practice in modern rail grinding, *Fatigue and Fracture of Engineering Materials and Structures* 26.10 (2003), 921–929.

[34] U. Olofsson and T. Telliskivi, Wear, plastic deformation and friction of two rail steels – a full-scale test and a laboratory study, *Wear* 254.1-2 (2003), 80–93.

[35] C. Paderno, Simulation of ballast behaviour under traffic and tamping process, 9th Swiss Transport Research Conference, Sept. 9–11 2009, Monte Verità/Ascona, Switzerland, 2009, 22 pp.

[36] P. Pointner, A. Joerg, and J. Jaiswal, *Definitive guideline on the use of different rail grades*, Report D4.1.5, INNOTRACK, 2009, 45 pp.

[37] *Question D 161, Final report – conclusions and recommendations*, Report, Utrecht, Netherland: Office for Research and Experiments of the International Union of Railways, 1988, 48 pp.

[38] *Railway applications – Track – Track geometry quality – Part 1:Characterisation of track geometry, EN 13848-1:2003+A1:2008 (E)*, European committee for standardization, 2008, 25 pp.

[39] *Railway applications – Track – Track geometry quality – Part 5:Geometric quality levels – Plain line, EN 13848-5:2008+A1:2010*, European committee for standardization, 2010, 22 pp.

[40] *Railway applications – Track – Track geometry quality – Part 6:Characterisation of track geometry quality, prEN 13848-6:22012*, European committee for standardization, 2012, 26 pp.

[41] *Recommendations for use of rail steel grades, Leaflet 721 (draft update 2012)*, UIC, 2012, 12 pp., URL: `http://www.uic.org`.

[42] S. Stichel et al., Investigation of the risk for rolling contact fatigue on wheels of different passenger trains, *Vehicle System Dynamics* 46.supp 1 (2008), 317–327.

[43] R. Stock et al., Influencing rolling contact fatigue through top of rail friction modifier application – a full scale wheel-rail test rig study, *Wear* 271.1-2 (2011), 134–142.

[44] *Strategier för drift och underhåll av väg- och järnvägsnätet*, in Swedish, Report, Vägverket, Banverket, Transportstyrelsen, and Sjöfartsverket, 2009, 140 pp.

[45] *Testing and approval of railway vehicles from the point of view of their dynamic behaviour – safety – track fatigue – running behaviour, Leaflet 518, 4th edn*, UIC, 2009, 126 pp., URL: `http://www.uic.org`.

[46] P. Torstensson, Rail corrugation growth on curves, PhD thesis, Department of Applied Mechanics, Chalmers University of Technology, 2012, 133 pp., ISBN: 978-91-7385-758-1.

[47] *Trials of wheel and rail rolling contact fatigue control measures – site monitoring and sustainable operation limits*, Report, London, UK: Rail Safety & Standards Board, 2010, 58 pp.

[48] J. Tunna and C. Urban, A parametric study of the effects of freight vehicles on rolling contact fatigue of rail, *Proceedings of the Institution of Mechanical Engineers, Part F: Journal of Rail and Rapid Transit* 223.2 (2009), 141–151.